Mutations in the *SPTLC2* Subunit of Serine Palmitoyltransferase Cause Hereditary Sensory and Autonomic Neuropathy Type I

Annelies Rotthier,[1,3,14] Michaela Auer-Grumbach,[4,14] Katrien Janssens,[1,3,14] Jonathan Baets,[2,3,5] Anke Penno,[6,7] Leonardo Almeida-Souza,[1,3] Kim Van Hoof,[1,3] An Jacobs,[1,3] Els De Vriendt,[2,3] Beate Schlotter-Weigel,[8] Wolfgang Löscher,[9] Petr Vondráček,[10] Pavel Seeman,[11] Peter De Jonghe,[2,3,5] Patrick Van Dijck,[12] Albena Jordanova,[2,3] Thorsten Hornemann,[6,13] and Vincent Timmerman[1,3,*]

Hereditary sensory and autonomic neuropathy type I (HSAN-I) is an axonal peripheral neuropathy associated with progressive distal sensory loss and severe ulcerations. Mutations in the first subunit of the enzyme serine palmitoyltransferase (SPT) have been associated with HSAN-I. The SPT enzyme catalyzes the first and rate-limiting step in the de novo sphingolipid synthesis pathway. However, different studies suggest the implication of other genes in the pathology of HSAN-I. Therefore, we screened the two other known subunits of SPT, *SPTLC2* and *SPTLC3*, in a cohort of 78 HSAN patients. No mutations were found in *SPTLC3*, but we identified three heterozygous missense mutations in the *SPTLC2* subunit of SPT in four families presenting with a typical HSAN-I phenotype. We demonstrate that these mutations result in a partial to complete loss of SPT activity in vitro and in vivo. Moreover, they cause the accumulation of the atypical and neurotoxic sphingoid metabolite 1-deoxy-sphinganine. Our findings extend the genetic heterogeneity in HSAN-I and enlarge the group of HSAN neuropathies associated with SPT defects. We further show that HSAN-I is consistently associated with an increased formation of the neurotoxic 1-deoxysphinganine, suggesting a common pathomechanism for HSAN-I.

Introduction

Hereditary sensory and autonomic neuropathy type I (HSAN-I [MIM 162400]) is an autosomal-dominant peripheral neuropathy presenting from the second decade of life onwards, with prominent sensory involvement and a variable degree of motor and autonomic dysfunction. The neurological phenotype is often complicated by severe infections, osteomyelitis, and amputations. On nerve conduction testing, sensory nerve action potentials are typically severely reduced to absent with relative preservation of nerve conduction velocities, classifying HSAN-I as an axonal neuropathy.[1–3]

HSAN-I has been reported to be associated with mutations in the first subunit (*SPTLC1* [MIM 605712]) of the enzyme serine palmitoyltransferase (SPT).[4–6] The SPT enzyme is a multisubunit structure, consisting of dimeric subunits of SPTLC1 with either SPTLC2 (MIM 605713) or SPTLC3 (MIM 611120).[7] It is associated with the endoplasmic reticulum (ER), where it catalyzes the pyridoxal-5′-phosphate (PLP)-dependent condensation of L-serine with palmitoyl-CoA. This is the first and rate-limiting step in the de novo biosynthesis of sphingolipids (Figure S1, available online).[8] Sphingolipids are essential components of all eukaryotic cells, with both structural and signaling functions. Mutations in a high number of enzymes involved in sphingolipid metabolism are associated with neurodegenerative diseases,[9] highlighting the importance of sphingolipids in neuronal functioning.

The HSAN-I-causing mutations in *SPTLC1* result in a significant reduction of SPT enzymatic activity, but the effects on total sphingolipid levels remain controversial.[5,10,11] It has been established, though, that the mutations cause a shift in substrate specificity: the mutant enzyme is able to incorporate, besides serine, alanine and glycine to form, respectively, 1-deoxysphinganine (1-deoxy-SA) and 1-deoxymethylsphinganine (1-deoxymethyl-SA) instead of sphinganine (SA).[12,13] These alternative metabolites show pronounced neurotoxic effects on neurite formation in cultured sensory neurons.[13]

Systematic screening of the known HSAN genes in a large series of patients yielded pathogenic mutations in only 19% of probands,[6] suggesting the involvement of other disease-associated genes. Because of the identification of missense mutations in the *SPTLC1* subunit of SPT in HSAN-I patients, we have sequenced the other SPT subunits *SPTLC2* and

[1]Peripheral Neuropathy Group, VIB Department of Molecular Genetics, University of Antwerp, B-2610 Antwerp, Belgium; [2]Neurogenetics Group, VIB Department of Molecular Genetics, University of Antwerp, B-2610 Antwerp, Belgium; [3]Laboratory of Neurogenetics, Institute Born-Bunge, University of Antwerp, B-2610 Antwerp, Belgium; [4]Department of Internal Medicine, Division of Endocrinology and Metabolism, Medical University of Graz, A-8036 Graz, Austria; [5]Department of Neurology, University Hospital Antwerp, B-2650 Antwerp, Belgium; [6]Institute for Clinical Chemistry, University Hospital Zurich, CH-8091 Zurich, Switzerland; [7]Competence Center for Systems Physiology and Metabolic Diseases, CH-8093 Zurich, Switzerland; [8]Friedrich-Baur-Institut, Department of Neurology Ludwig-Maximilians-University of Munich, D-80336 Munich, Germany; [9]Department of Neurology, Innsbruck Medical University, A-6020 Innsbruck, Austria; [10]Department of Paediatric Neurology, University Hospital and Masaryk University, CZ-613 00 Brno, Czech Republic; [11]Department of Child Neurology, Charles University, 2nd School of Medicine Prague, CZ-150 06 Prague, Czech Republic; [12]VIB Department of Molecular Microbiology, Laboratory of Molecular Cell biology, University of Leuven, B-3001 Leuven, Belgium; [13]Institute of Physiology and Zurich Center for Integrative Human Physiology (ZIHP), University of Zurich, CH- 8057 Zurich, Switzerland
[14]These authors contributed equally to this work
*Correspondence: vincent.timmerman@molgen.vib-ua.be
DOI 10.1016/j.ajhg.2010.09.010.

SPTLC3 as functional candidate genes in a large HSAN cohort. In this study, we report three heterozygous missense mutations in *SPTLC2* in four index patients presenting with HSAN-I. In in vitro assays as well as in a yeast complementation assay, we found that the mutations reduce SPT activity. Additional characterization shows that the three mutations cause the formation of the neurotoxic metabolite 1-deoxy-SA in human embryonic kidney (HEK) 293 and patient lymphoblast cells. Together with previously reported findings of HSAN-I-causing *SPTLC1* mutations, our results indicate that mutations in the two SPT subunits cause a common HSAN pathomechanism.

Subjects and Methods

Subjects

For this study, we selected a group of 78 patients with hereditary ulceromutilating and sensory neuropathies. Our inclusion criteria were described previously in Rotthier et al.[6] Prior to enrollment in this study, all patients or their legal representatives provided informed consent of participation to the treating physicians. This study was approved by the local institutional review board.

Mutation Analysis

All DNA samples were amplified with the use of the whole-genome amplification kit GenomiPhi V2 DNA Amplification Kit (GE Healthcare). The coding regions and exon-intron boundaries up to 100 bp up- and downstream of the exons of *SPTLC2* and *SPTLC3* were amplified via PCR with the use of oligonucleotide primers designed with the Primer3 and SNPbox software tools.[14,15] Primer sequences are listed in Tables S1 and S2. Mutation screening was performed by direct DNA sequencing of purified PCR fragments with the use of the BigDye Terminator v3.1 Cycle Sequencing Kit (Applied Biosystems) and separation on an ABI3730xl DNA Analyzer (Applied Biosystems). The resulting sequences were aligned and analyzed with the novoSNP[16] and SeqMan II programs. Sequence variants were confirmed by repeated PCR on original DNA samples and bidirectional sequencing.

Parenthood was tested with the use of 15 highly informative short tandem repeats (STRs) distributed throughout the genome (ATA38A05, D1S1646, D1S1653, D1S1360, D2S2256, D3S3037, D4S2382, D4S3240, D7S509, D8S1759, D9S1118, D12S1056, D12S2082, D16S2619, and GATA152H04). STRs were amplified via PCR, and PCR fragments were loaded on an ABI3730xl DNA Analyzer. Genotypes were analyzed with Local Genotype Viewer.

Cloning

The *SPTLC2* cDNA (NM_004863.2) was amplified and cloned into the Gateway entry vector pDONR221 (Invitrogen) with the use of the primers SPTLC2_attb1 and SPTLC2_attb2. The *SPTLC2* mutations were introduced by site-directed mutagenesis, with the use of the following primers: SPTLC2_V359M_fw, SPTLC2_V359M_rv, SPTLC2_G382V_fw, SPTLC2_G382V_rv, SPTLC2_I504F_fw, and SPTLC2_I504F_rv. Primer sequences can be found in Table S3.

The constructs were recombined in the destination vector pEF5/FRT/V5-DEST (Invitrogen), fusing the cDNA with a C-terminal V5 tag. All constructs were validated by sequencing. Stable cell lines were generated with the use of the Flp-in host cell line HEK293 in accordance with the manufacturer's instructions (Invitrogen).

Yeast *LCB2* together with its own promotor (700 bp upstream of the start codon) and own terminator (450 bp downstream of the stop codon) was cloned into the YCplac111 plasmid vector, harboring a LEU2 gene. Mutations and an HA tag were introduced by site-directed mutagenesis with the use of the primers LCB2_HA_fw, LCB2_HA_rv, LCB2_V346M_fw, LCB2_V346M_rv, LCB2_G369V_fw, LCB2_G369V_rv, LCB2_I491F_fw, LCB2_I491F_rv, LCB2_K366T_fw, and LCB2_K366T_rv. Primer sequences are listed in Table S3.

Cell Culture Material and Conditions

HEK293 Flp-in cells were cultivated at 37°C and 5% CO_2 in Dulbecco's modified Eagle's medium supplemented with 10% fetal bovine serum (FBS), L-glutamine, and penicillin and streptomycin. Lymphoblastoid cell lines were cultured at 37°C and 5% CO_2 in Roswell Park Memorial Institute medium (RPMI) supplemented with 10% FBS, L-glutamine, sodium pyruvate, and penicillin and streptomycin. All cell culture media and supplements were from Invitrogen.

Lymphoblastoid Cell Lines

Total blood samples were mixed with 15 ml of Ficol Paque and centrifuged for 10 min. After washing, lymphocytes were transformed with Epstein-Barr virus and incubated at 37°C for 2 hr. After centrifugation, the pellet was resuspended in 4 ml RPMI complete medium + 1% phytohaemagglutinin. Cells were seeded in a 24-well plate and incubated at 37°C and 5% CO_2 for a minimum of 3 days. Cells were split and supplemented with fresh medium as needed.

Yeast Complementation Assay

The YCplac111 constructs containing wild-type (WT) or mutant *LCB2* were transformed[17] in a heterozygous LCB2 deletion strain (BY4743), in which LCB2 has been replaced by a kanamycin-resistance gene, and sporulated. The resulting tetrads were dissected for the generation of haploid spores that lack endogenous expression of LCB2, and they were grown on YPD medium with phytosphingosine (15 μM; Avanti Polar Lipids) and 0.1% tergitol at 26°C. After two days, replica plating to different growth media was performed, namely YPD medium at 18°C and 37°C (yeast SPT mutants have a thermosensitive growth phenotype[18]), synthetic minimal medium without leucine (allowing for selection of transformed spores), and YPD medium with geneticin (selection of LCB2-deficient spores). For each construct, at least six tetrads were analyzed. Unless specified otherwise, media and supplements were from Sigma.

RNA Isolation and mRNA Analysis

Total mRNA was purified with the RNeasy Mini Kit (Qiagen). DNA inactivation was performed with the Turbo DNA-free Kit (Ambion), and cDNA synthesis was performed with Superscript III First-Strand Synthesis System for RT-PCR (Invitrogen). Expression of SPTLC2 (endogenous and construct) was analyzed with the use of the following primer combinations: SPTLC2_Fw: 5′-GAGTCCA GAGCCAGGTTTTG-3′ and SPTLC2_3′UTR_Rv: 5′-CTGAGGGAG CACCAAAAAG-3′ (for endogenous SPTLC2 expression) or V5_Rv: 5′-GAGAGGGTTAGGGATAGGCTTAC-3′ (for SPTLC2 construct).

Real-time quantitative PCR (RT-qPCR) reactions were performed in triplicate with 10 ng cDNA in SYBR Green I mix (Applied Biosystems) and run on an ABI Prism 7900HT Sequence Detection System (Applied Biosystems). Primers were validated for specificity

and amplification efficiency. RT-qPCR data were normalized according to the method described by Vandesompele et al.[19] The relative expression levels were used to normalize the data of the Fumonisin B1 block assay, the in vitro SPT activity assay, and the 1-deoxy-SA quantification.

Fumonisin B1 Block Assay

This assay was performed as described in Penno et al.[13] In brief, Fumonisin B1 (Sigma) was added to the media of exponentially growing cells in a final concentration of 10 μg/ml. As a negative control, the SPT inhibitor myriocin (10 μg/ml, Sigma) was added together with Fumonisin B1. 24 hrs after Fumonisin B1 addition, cells were washed twice with PBS, harvested, and counted (Coulter Z2, Beckman Coulter). Next, the cells were subjected to lipid extraction under basic conditions (see below). Sphingoid bases were quantified by liquid chromatography-mass spectrometry (LC-MS). Synthetic C17 sphingosine (Avanti Polar Lipids) was added to each sample as an internal extraction standard.

In Vitro Radioactivity-Based SPT Activity Assay

SPT activity was measured with the use of the radioactivity-based assay described by Rütti et al.[20] In brief, 400 μg total cell lysate, 50 mM HEPES (pH 8.0), 0.5 mM L-serine, 0.05 mM Palmitoyl-CoA, 20 μM Pyridoxal-5′-phosphate, 0.2% sucrose monolaureate (all from Sigma), and 0.1 μCi L-[U-14C] serine (Amersham) were mixed and incubated at 37°C. In the control reaction, SPT activity was specifically blocked by the addition of myriocin (40 μM, Sigma). After 60 min, the reaction was stopped and lipids were extracted according to the method of Riley et al.[21] (see below).

Lipid Extraction and Hydrolysis

Total lipids were extracted from cells or plasma according to the method of Riley et al.[21] For acid hydrolysis, the dried lipids were resuspended in 200 μl methanolic HCl (1N HCl/10M water in methanol) and kept at 65°C for 12–15 hrs. The solution was neutralized by the addition of 40 μl KOH (5M) and subsequently subjected to base hydrolysis, which was performed as follows: 0.5 ml extraction buffer (4 vol. 0.125M KOH in methanol + 1 vol. chloroform) was added to the solution. Subsequently, 0.5 ml chloroform, 0.5 ml alkaline water, and 100 μl 2M ammonia were added in that order. Liquid phases were separated by centrifugation (12,000 g, 5 min). The upper phase was aspirated and the lower phase washed twice with alkaline water. Finally, the lipids were dried by evaporation of the chloroform phase under nitrogen gas and subjected to LC-MS analysis.

Extracted lipids were solubilized in 56.7% methanol-33.3% ethanol-10% water and derivatized with ortho-phtalaldehyde. The lipids were separated on a C18 column (Uptispere 120 Å, 5 μm, 125 × 2 mm, Interchim, France) fluorescence detector (HP1046A, Hewlet Packard) followed by detection on an MS detector (LCMS-2010A, Shimadzu). Atmospheric pressure chemical ionization was used for ionization. Nonnatural C17 sphingosine (Avanti Polar Lipids) was used as internal standard. Retention times were as follows: C_{17}SO (internal standard): 6 min; sphingosine: 7.5 min; 1-deoxysphingosine: 9 min; 1-deoxymethylsphingosine: 10.5 min; SA: 10.5 min; 1-deoxymethyl-SA: 13 min; 1-deoxy-SA: 13.5 min. MS data were analyzed with the use of LCMS solution (Shimadzu) and MS Processor v.11 (ACD Labs).

Statistics

The two-tailed unpaired Student's t test was used for statistical analysis. Error bars (standard deviation) and p values (Student's t test) were calculated on the basis of three independent experiments.

Results

Mutations in *SPTLC2* Are Associated with HSAN-I

The coding sequence and intron-exon boundaries of *SPTLC2* (chromosome location 14q24.3) were analyzed in 78 patients with HSAN who had been previously screened and found to be negative for mutations in the other known HSAN genes (*SPTLC1, RAB7* [MIM 602298], the complete coding region of *WNK1/HSN2* [MIM 605232], *FAM134B* [MIM 613114], *NTRK1* [MIM 191315], *NGFB* [MIM 162030], and *CCT5* [MIM 610150]).[6,22] We identified three heterozygous missense mutations in four index patients, for whom clinical and electrophysiological information is summarized in Table 1 and Table 2. The mutations were absent in 300 European control individuals.

A c.1145G>T sequence variation (p.G382V) was found in two families (CMT-1044 and CMT-1117; Figure 1A). The proband of family CMT-1117 presented with progressive distal sensory loss and distal muscle weakness in the lower limbs at the age of 38 yrs. The clinical presentation was similar in a member of family CMT-1044. In addition, this patient experienced dysesthesia in hands and feet and developed osteomyelitis of a thumb. On the basis of haplotype analysis, these families were found to be unrelated (data not shown).

A second heterozygous mutation (c.1075G>A [p.V359M]) was discovered in an isolated patient (CMT-747.I:1; Figure 1B). This patient was diagnosed with HSAN after developing distal sensory dysfunction with a foot ulceration necessitating amputation of a toe. No signs of motor or autonomic involvement were noted.

The third mutation (c.1510A>T [p.I504F]) is a heterozygous de novo mutation found in patient CMT-635.II:1, who presented with an atypical early-onset sensorimotor neuropathy complicated with ulcerations, osteomyelitis, and anhidrosis (Figures 1C and 1D). Paternity testing was performed for confirmation of parenthood.

Nerve conduction studies were performed in all patients, revealing predominantly axonal sensorimotor neuropathy; this diagnosis was confirmed by a sural nerve biopsy in patient CMT-747.I:1 (Table 1 and Table 2).

No disease-associated sequence variants were identified in the coding region or the intron-exon boundaries of *SPTLC3* (chromosome location 20p12.1).

SPTLC2 Mutations Are Associated with a Reduction in SPT Activity

All three mutations in *SPTLC2* target highly conserved amino acids (Figure 2A), rendering it likely that they are functionally important. We set out to investigate the effect

Table 1. Clinical Features of Patients with *SPTLC2* Mutation

Origin	FH	AO	Pres. Sym.	Dis. Dur.	Ulc.	Ost.	Amp.	Sen. Dys.	Aut. Dys.	Dist. Wkn.	NCS	Additional
Patient: CMT-747.I:1; Mutation: c.1075G>A (p.V359M)												
Austria	IC	52 yrs	ulceration and amputation of great R toe	27 yrs	+ (toes)	+	+	+ (distal LL)	-	-	axonal/ intermediate sensorimotor	sural nerve biopsy: axonal neuropathy in particular of unmyelinated fibers
Patient: CMT-1044.I:2; Mutation c.1145G>T (p.G382V)												
Germany	D	37 yrs	dysesthesia and sensory loss, distal UL and LL	35 yrs	-	+ (thumb R)	-	+ severe distally panmodal with dysesthesia	-	+ UL (0-3/5) and LL (0/5)	axonal/ intermediate sensorimotor	scoliosis, focal epilepsy; brisk reflexes UL; clenched hand R > L
Patient: CMT-1117.II:1; Mutation: c.1145G>T (p.G382V)												
Austria	D	38 yrs	sensory loss in feet	8 yrs	-	-	-	+ distally for touch and vibration	-	+ LL (2/5)	axonal sensorimotor	-
Patient: CMT-1117.I:2; Mutation c.1145G>T (p.G382V)												
Austria	D	?	asymptomatic	?	-	-	-	+ distally LL for vibration	-	+ LL (5-/5)	axonal sensorimotor	type 2 diabetes (onset: 71 yrs)
Patient: CMT-635.II:1; Mutation c.1510A>T (p.I504F)												
Czech Republic	IC (de novo)	5 yrs	gait difficulties, foot deformities	9 yrs	+ (LL)	+	-	+	+	+ (LL)	intermediate sensorimotor	-

FH, familial history; AO, age at onset; Pres. Sym., present symptom(s); Dis. Dur., disease duration; Ulc., ulceration; Ost., osteomyelitis; Amp., amputation; Sen. Dys., sensory dysfunction; Aut. Dys., autonomic dysfunction; Dist. Wkn., distal weakness; NCS, nerve conduction studies; IC, isolated case; R, right; L, left; LL, lower limbs; UL, upper limbs; D, dominant; +, present; -, absent; ?, unknown. For distal weakness, the Medical Research Council scale (0, 1-, 1, 1+, …, 5-, 5) is shown in parentheses, indicating the severity of muscle weakness.

of these mutations on SPT activity in stably transfected Flp-in HEK293 cells. The Flp-in system ensures the stable insertion of a single copy of the transgene at a specific genomic location. In this way, moderate and equal expression of the different transgenes is obtained. The cells were treated for 24 hr with Fumonisin B1, a mycotoxin that blocks the de novo sphingolipid biosynthesis pathway downstream of SPT[23] (Figure S1). Because condensation of palmitoyl-CoA and serine by SPT is the rate-limiting step in the biosynthesis pathway, the resulting accumulation of SA reflects the canonical SPT activity (incorporation of L-serine). Stable expression of WT SPTLC2 resulted in an

Table 2. Nerve Conduction Studies in Patients with *SPTLC2* Mutation

			Median M		Ulnar M		Peroneal M		Tibial M		Median S		Ulnar S		Sural S	
Patient	**Age**	**R/L**	**Amp**	**CV**	**Amp**	**CV**	**Amp**	**CV**	**Amp**	**CV**	**Amp**	**CV**	**Amp**	**CV**	**Amp**	**CV**
Normal values ≥			**4.0**	**49.0**	**4.0**	**49.0**	**3.0**	**41.0**	**3.0**	**41.0**	**7.0**	**46.0**	**2.0**	**47.0**	**1.0**	**44.0**
CMT-747.I:1	79 yrs	R	9.7	*44.3*	-	-	*0.1*	*35.7*	-	-	*A*	*A*	-	-	-	-
		L	8.4	51.0	-	-	*0.1*	*23.3*	-	-	*0.9*	*35.2*	-	-	-	-
CMT-1044.I:2	72 yrs	R	*0.1*	*34.0*	*0.5*	*37.0*	*A*	*A*	*A*	*A*	*A*	*A*	*A*	*A*	*A*	*A*
CMT-1117.II:1	44 yrs	R	6.2	*55.0*	-	-	*A*	*A*	*A*	*A*	*A*	*A*	*0.4*	*38.0*	*A*	*A*
CMT-1117.I:2	72 yrs	R	9.9	*47.0*	5.6	51.0	3.0	42.0	-	-	-	-	-	-	2.7	*33.0*
CMT-635.II:1	14 yrs	R	*3.8*	*25.0*	*2.9*	50.0	*A*	*A*	*A*	*A*	*A*	*A*	*A*	*A*	*A*	*A*
		L	*2.0*	*29*	*2.1*	53	*A*	*A*	*A*	*A*	-	-	-	-	-	-

M, Motor; S, Sensory; Age, age at clinical examination; Amp, amplitude of the nerve action potential (motor: mV; sensory: μV); CV, conduction velocity (in m/s); A, absent response; -, not measured; R, right; L, left. Italics indicate abnormal values.

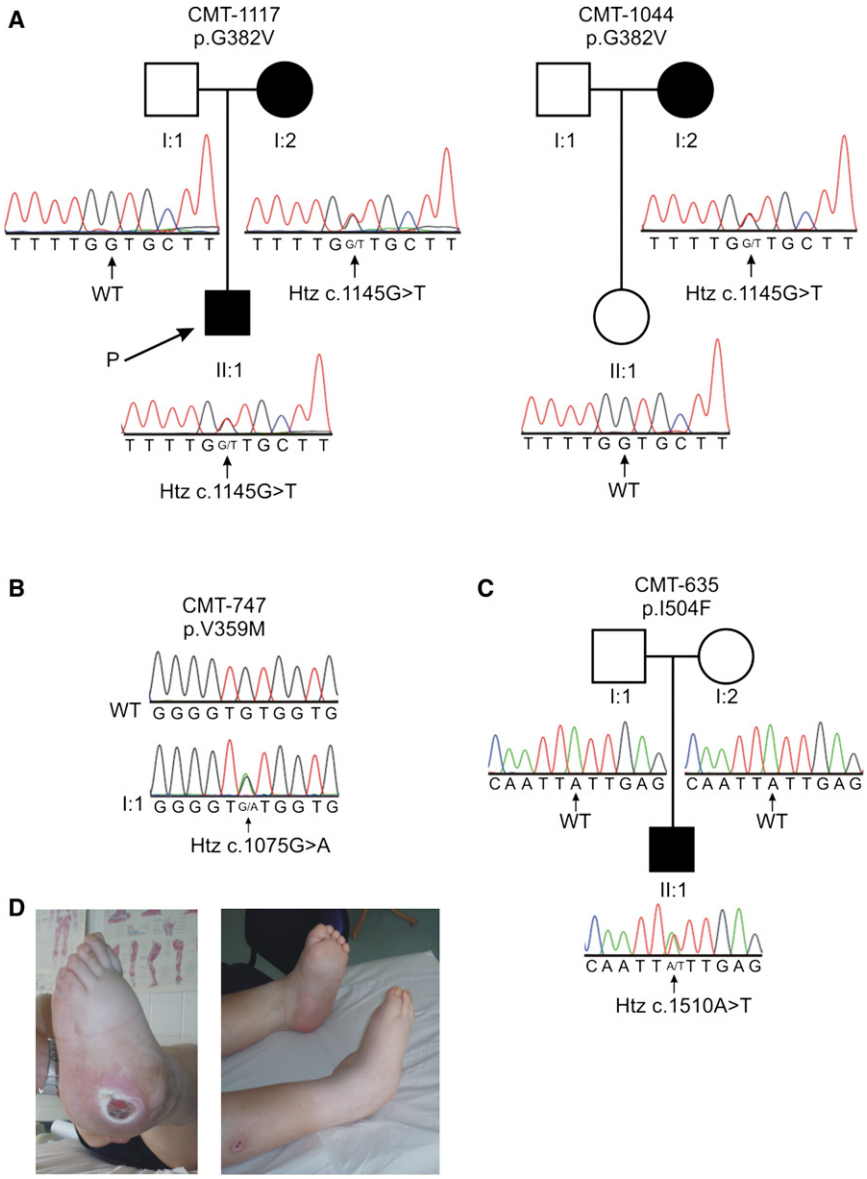

Figure 1. Missense Mutations in *SPTLC2* Are Associated with HSAN-I

(A) Sequence trace files of the G382V mutation in families CMT-1117 (proband indicated by arrow) and CMT-1044.

(B) Isolated patient CMT-747.I:1 with the V359M mutation.

(C) Patient CMT-635.II:1 carrying a de novo I504F mutation.

(D) Severe ulcerations and deformation of the foot of patient CMT-635.II:1 at the age of 10 yrs.

Htz, heterozygous; WT, wild type.

8-fold increase in SA accumulation as compared to control cells stably expressing green fluorescent protein (GFP). This is in agreement with earlier reports, in which overexpression of WT SPTLC2 indeed leads to higher SPT activity.[24] Stable expression of the G382V mutant, on the other hand, did not increase SA accumulation above basal levels. The V359M- and I504F-expressing cells showed an increase in SA accumulation, although far less pronounced than that of WT SPTLC2-expressing cells (Figure 3A). Thus, the three mutations result in a partial to complete loss of SPT activity.

The effect on canonical SPT activity was confirmed in an alternative radioactive-based in vitro assay. Total lipids were extracted from HEK293 cells stably expressing WT or mutant SPTLC2 and incubated with ^{14}C-labeled L-serine, PLP, and palmitoyl-CoA, after which the incorporation of the radioactively labeled serine was measured (Figure 3B). The results resembled those of the previous assay. Stable expression of WT SPTLC2 caused a significant increase in SPT activity, whereas the expression of G382V failed to raise SPT activity above basal levels. Expression of the V359M or I504F mutant elevated SPT activity, but not to the same extent as WT SPTLC2. The relative increase in SPT activity in V359M- and I504F-expressing cells was more pronounced than in the Fumonisin B1 block assay (Figure 3A). This difference could be explained by the higher serine concentration used in the latter in vitro assay in comparison to the serine concentrations present in the cell culture medium during the former assay.

SPTLC2 Mutants Differentially Affect In Vivo SPT Activity in *S. cerevisiae*

To corroborate the loss of canonical SPT activity in vivo, we expressed the corresponding yeast mutants (Figure 2A) in a heterozygous *LCB2* deletion yeast strain (*LCB2* is the *S. cerevisiae* ortholog of *SPTLC2*) and performed a tetrad analysis in order to obtain two haploid spores with and two without endogenous LCB2. As expected, all four spores grow at the permissive temperatures of 18°C, regardless of whether they express WT or mutant LCB2. At the restrictive temperature (37°C), spores with (residual) SPT activity will be able to grow, whereas spores with no or nonfunctional LCB2 will depend on the external addition of phytosphingosine in order to generate phytosphingolipids and grow.[18] WT LCB2 was able to complement the LCB2 deficiency, as apparent from the appearance of four equally sized colonies in the absence of phytosphingosine (Figure 4). In contrast, but analogous to the dominant-negative LCB2 K366T mutation,[25] yeast spores expressing the G369V mutation (corresponding to G382V in SPTLC2) yielded only colonies when endogenous LCB2 was present, demonstrating the failure of this mutant to complement LCB2 deficiency. The residual activity conferred by the V346M and I491F mutants (corresponding to V359M

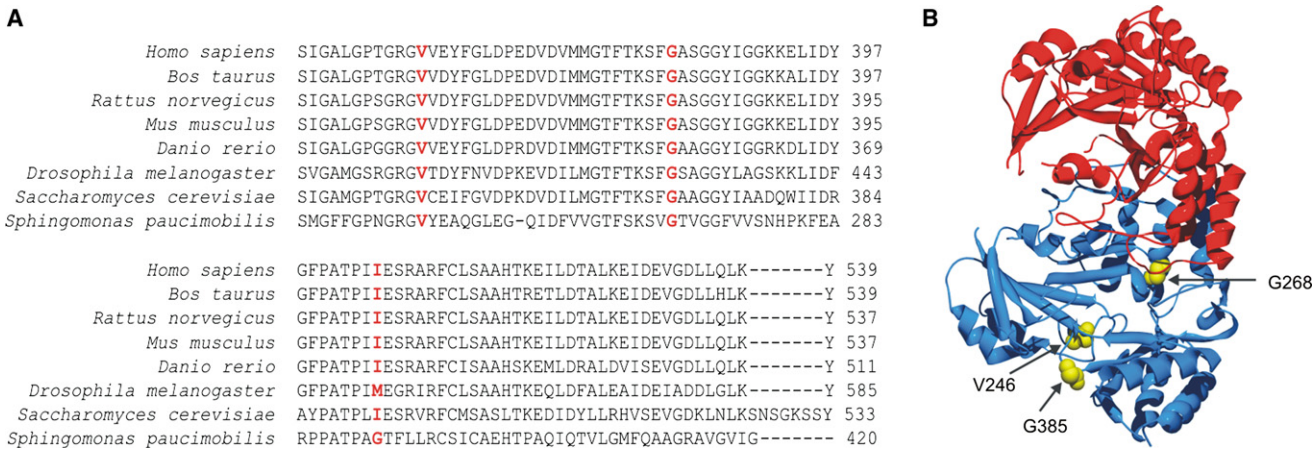

Figure 2. Conservation of Mutations among Species and Structural View of the Bacterial SPT Enzyme
(A) ClustalW multiple protein alignment of the SPTLC2 orthologues from human (*Homo sapiens*), mouse (*Mus musculus*), rat (*Rattus norvegicus*), taurus (*Bos Taurus*), zebrafish (*Danio rerio*), fly (*Drosophila melanogaster*), baker's yeast (*Saccharomyces cerevisiae*), and Gram-negative bacteria with SPT activity (*Sphingomonas paucimobilis*).
(B) SPT structure of the *Sphingomonas paucimobilis* SPT homodimer (PDB ID: 2JGT) with the dimeric subunits represented in red and blue. The highlighted amino acids (V246, G268, and G385) correspond to the amino acids (V359, G382, and I504) mutated in the HSAN-I patients (see alignment in A).

and I504F, respectively, in SPTLC2) was sufficient to restore growth at 37°C; this is in accordance with our biochemical data.

Mutant SPT Shows Ambiguity towards Its Amino Acid Substrate

A recent report shows that SPTLC1 mutations in HSAN-I influence the substrate specificity of the SPT enzyme: mutant SPT is able to metabolize L-alanine and to a lesser extent glycine as alternative substrates. This results in the formation of the atypical and neurotoxic sphingoid base metabolites 1-deoxy-SA and 1-deoxymethyl-SA.[12,13] The accumulation of these metabolites in the peripheral nerves was postulated to be the underlying cause of HSAN-I.[13] To study whether SPTLC2 mutations likewise affect the enzymatic affinity of SPT and cause a similar accumulation of these alternative metabolites, we analyzed the sphingoid base profile of HEK293 cells expressing the mutants. In cells stably expressing WT SPTLC2, the amount of 1-deoxy-SA was similar to control cells (Figure 5A), showing that an increase in SPT activity as such does not alter substrate specificity. Expression of the mutants, on the other hand, resulted in up to 20-fold higher 1-deoxy-SA levels in comparison to control cells, the highest levels in HEK cells stably expressing the G382V or I504F mutant enzyme. The generation of 1-deoxymethyl-SA levels in both HEK cells and lymphoblast cells was below detection limits.

To validate whether the results obtained in the HEK cells reflect the situation in HSAN-I patients, we measured 1-deoxy-SA levels in lymphoblast cell lines from two HSAN-I patients carrying, respectively, the G382V and I504F mutation. In both cell lines, accumulation of 1-deoxy-SA was observed when compared to unaffected family members or unrelated healthy control individuals (Figure 5B). This finding is in agreement with our in vitro results and, more importantly, shows that the accumulation of 1-deoxy-SA could be physiologically relevant.

Discussion

We previously reported that only 19% of a cohort of 100 HSAN patients had mutations in the coding regions of genes known to be mutated in HSAN, suggesting additional genetic heterogeneity.[6] This was strengthened by our recent identification of *FAM134B* mutations in HSAN-II (MIM 613115) patients from this cohort.[22] Because mutations in the first subunit of SPT were found to be associated with HSAN-I,[4–6] we screened the two other subunits of SPT, *SPTLC2* and *SPTLC3*, as functional candidate genes in 78 patients with hereditary ulceromutilating and sensory neuropathies. This cohort shows a wide variability of clinical features and different modes of inheritance, but all patients share a progressive distal sensory dysfunction. The functional candidate approach has been proven to be valuable, especially in the case of rare, debilitating disorders, in which small pedigrees preclude the use of classical positional cloning. Although mutations in *SPTLC2* were previously excluded as a common cause of HSAN-I,[26] we still supported the strength of this gene as a functional candidate gene for HSAN. This was based on the reported effects of the *SPTLC1* mutations, namely a reduction in SPT activity and the accumulation of atypical sphingolipid metabolites; both effects could be envisaged as resulting from mutations in the other SPT subunits as well.

No disease-associated mutations were identified in the third subunit of SPT (*SPTLC3*) in our HSAN cohort. It was

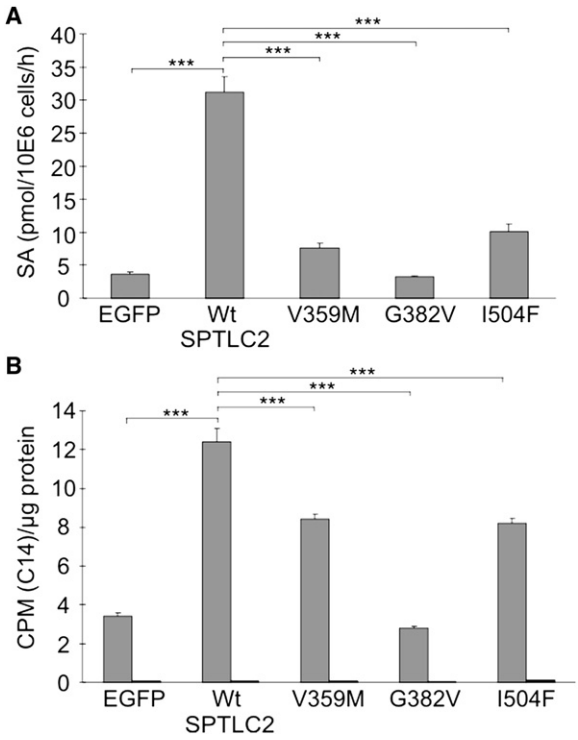

Figure 3. In Vitro SPT Activity Measurements of HSAN-I Associated SPTLC2 Mutants

(A) Fumonisin B1 block assay. SPT activity in HEK293 cells stably expressing WT or mutant SPTLC2 is analyzed by measuring SA accumulation after treatment with Fumonisin B1. Stable expression of WT SPTLC2 generates an 8.5-fold increase in SPT activity ($p = 3.24 \times 10^{-5}$), whereas the G382V mutant does not increase SPT activity ($p = 0.18$). The V359M and I504F mutations increase the activity significantly ($p = 0.00063$ and 0.00064, respectively) but not to the same extent as WT SPTLC2. Enhanced GFP (EGFP)-transfected cells served as control.

(B) Radioactivity-based SPT activity assay. SPT activity of HEK293 cells stably expressing WT or mutant SPTLC2 was determined by measuring the incorporation of ^{14}C-labeled L-serine in vitro. Stable expression of WT SPTLC2 results in a significant increase in SPT activity, whereas the expression of G382V fails to raise SPT activity above basal levels. Expression of the V359M or I504F mutant elevates SPT activity, but not as drastically as WT SPTLC2. The right bars represent SPT activity in the presence of the SPT inhibitor myriocin (negative control; see Figure S1).

CPM, counts per minute; SA, sphinganine. *** $p < 0.001$. Data are represented as mean, with error bars representing standard deviations. Error bars and standard deviation were calculated on the basis of three independent experiments.

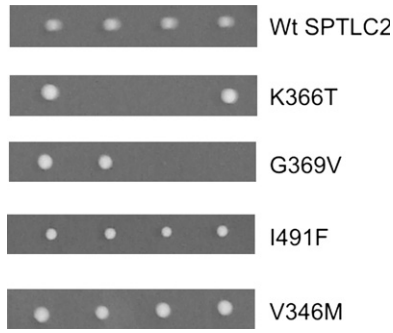

Figure 4. Genetic Complementation Test in *S. cerevisiae* by Tetrad Dissection of a Heterozygous *LCB2/lcb2::KanMX* Strain Complemented with Different YCplac111_LCB2 Constructs

WT LCB2 can complement LCB2 deficiency, as shown by the appearance of four equally sized colonies on YPD medium without phytosphingosine at 37°C. The V346M (corresponding to V359M in SPTLC2) and I491F (corresponding to I504F in SPTLC2) LCB2 mutants also rescue the absence of endogenous LCB2. However, yeast transformed with the G369V (corresponding to G382V in SPTLC2) or K366T (dominant negative) mutants yields only colonies when endogenous LCB2 is present, demonstrating the failure of these mutants to complement LCB2 deficiency.

previously suggested that SPTLC2 and SPTLC3, which are isoforms, allow for the adjustment of SPT activity to tissue-specific requirements for sphingolipid synthesis.[24] Given the low expression levels of SPTLC3 in neuronal tissue,[24] SPTLC3 is indeed unlikely to have a role in neurological diseases. Although we cannot completely rule out mutations in *SPTLC3*, we exclude mutations in this gene as a common cause for HSAN.

In *SPTLC2*, we identified three missense mutations—V359M, G382V, and I504F—in patients diagnosed with HSAN-I. The patients carrying the V359M (CMT-747.I:1) and G382V (CMT-1117.II:1 and CMT-1044.I:2) mutations had a very similar disease course, with adult onset of prominent sensory dysfunction and variable motor involvement. The mother of CMT-1117.II:1, CMT-1117.I:2, who also carries the G382V mutation, presents with a mild peripheral neuropathy that was noticed only upon clinical examination. Because this patient was diagnosed with a mild form of diabetes, the origin of the peripheral neuropathy in this patient is debatable. Of note, many inherited peripheral neuropathies are associated with a very broad phenotypic variability, both inter- and intrafamilial, rendering it well possible that patient CMT-1117.I:2 is indeed an asymptomatic carrier of this mutation. In our opinion, this by no means casts doubt on the pathogenicity of the mutation, given that we provided strong functional evidence for its causative role in HSAN-I (further discussed below).

The patient with the de novo I504F mutation was phenotypically distinct, the most remarkable difference being the onset of the disease in childhood. Moreover, this patient also experienced autonomic dysfunction, namely sweating disturbances. It is noteworthy that the S331F mutation in *SPTLC1* is also associated with an atypical and early-onset HSAN-I phenotype.[6] These two observations clearly illustrate that the phenotypic spectrum of this rare disorder is broad and warrants the inclusion of patients with an early disease onset (< 10 yrs) in future screenings for *SPTLC* mutations. Furthermore, the identification of a second gene for HSAN-I and the presence in our cohort of HSAN-I patients without mutation in either of the two known genes demonstrate the genetic heterogeneous nature of this disorder and call for a further screening of functional candidate genes, such as the recently identified regulatory interactors of SPT, the small

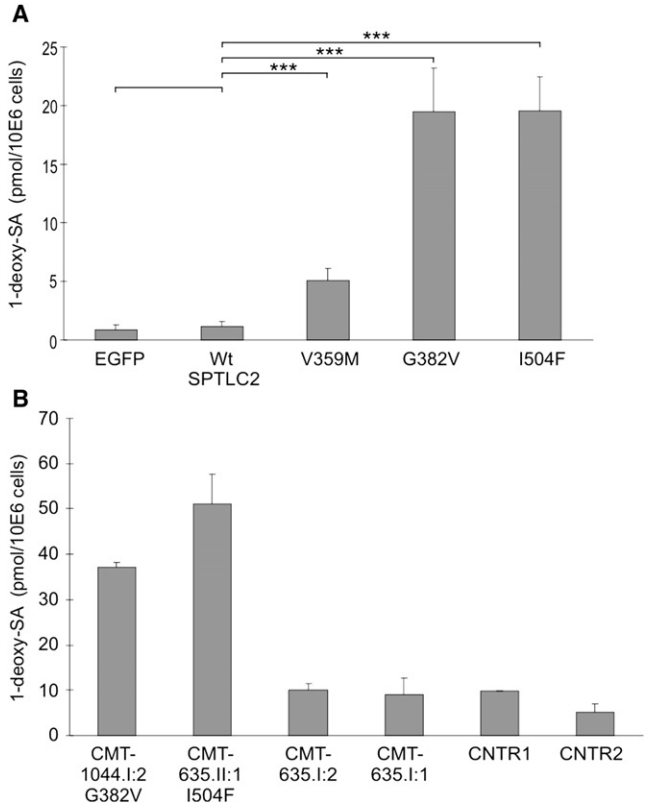

Figure 5. SPTLC2 Mutations Affect the Enzymatic Affinity of SPT
(A) Levels of 1-deoxy-SA in HEK293 cells stably expressing WT or mutant SPTLC2 are measured after an acid and base hydrolysis assay of the extracted lipids. Expression of WT SPTLC2 does not change cellular 1-deoxy-SA levels ($p = 0.55$), whereas all three HSAN-I-associated mutants result in significantly elevated 1-deoxy-SA levels ($p = 0.0025$ for V359M; 0.00093 for G382V; 0.00048 for I504F).
(B) 1-deoxy-SA levels in HSAN-I patient lymphoblastoid cell lines. The two HSAN-I patients CMT-1044.I:2 (G382V mutation) and CMT-635.II:1 (I504F mutation) show higher levels of 1-deoxy-SA compared to the unaffected parents of CMT-635.II:1 and to two unrelated control individuals. Unfortunately, no lymphoblast cells were available of patient CMT-747.I:1 carrying the V359M mutation.
*** p value < 0.001. SA, sphinganine. Data are represented as mean, with error bars representing standard deviations. Error bars and standard deviation were calculated on the basis of three independent experiments.

stimulatory SPT subunits (ssSPT)[27] and the ORMDL proteins.[28,29]

The three disease-associated mutations identified in this study target highly conserved amino acids residing in conserved domains, possibly indicating functionally important domains. In particular, the G382 residue is an active residue in the putative PLP-binding domain of SPTLC2.[30] A study by Gable et al.[25] suggests that the known HSAN-I associated SPTLC1 mutations (C133W, C133Y, V144D) indirectly affect PLP binding by altering the geometry of the PLP-binding site in the dimeric conformation. They tested their hypothesis by mutating amino acids in the putative PLP-binding domain in LCB2, the yeast ortholog of SPTLC2. In support of their assumption, the mutations dominantly inactivated SPT activity, suggesting that mutations in the PLP-binding domain of *SPTLC2* could cause a phenotype similar to HSAN-I caused by *SPTLC1* mutations. On the basis of these observations, together with the reported decrease of SPT activity for HSAN-I-associated *SPTLC1* mutations, the effect of our *SPTLC2* mutations on SPT activity was not unexpected. Interestingly, however, the three mutations have a differential effect on the canonical enzymatic activity. In two independent in vitro assays, the expression of G382V fails to raise SPT activity above basal levels, whereas expression of the V359M or I504F mutant confers limited SPT activity. This duality is also observed in an in vivo assay: the yeast mutant corresponding to G382V is unable to complement the absence of endogenous LCB2, whereas the partial activity retained by the two other mutants suffices to allow growth. It is possible that the position of the affected amino acids accounts for the differential effect of the mutations on SPT activity: the structure of the bacterial (*Sphingomonas paucimobilis*) SPT homodimer shows that the G268 residue (corresponding to G382) resides in the putative interface between SPTLC1 and SPTLC2, the catalytic domain of SPT, whereas the other two mutated residues (V246 and G385, corresponding to V359 and I504) are located on the surface of the protein (Figure 2). Like WT SPTLC2 protein, mutant SPTLC2 colocalizes with the ER marker calreticulin in SH-SY5Y neuroblastoma cells (data not shown), rendering it unlikely that mislocalization of the mutant protein causes the loss in SPT activity.

Heterozygous Sptlc2 knockout mice, who have only one copy of SPTLC2, are not known to develop a neuropathy,[31] rendering it unlikely that haploinsufficiency is sufficient to cause the disease. Therefore, we set out to further characterize the effect of the mutations on SPT properties. Recently, the HSAN-I-associated mutations in *SPTLC1* were found to cause the accumulation of the neurotoxic metabolites 1-deoxy-SA and 1-deoxymethyl-SA. This is due to a shift in substrate specificity of mutant SPT that leads to the condensation of palmitoyl-CoA with alanine and glycine, besides serine.[13] Because these 1-deoxy bases lack the C_1 hydroxyl group (Figure S1), they can neither be degraded nor be converted into complex sphingolipids by the enzymes of the sphingolipid biosynthesis pathway; hence, they accumulate in the cell. In our study we found all three *SPTLC2* mutations to be associated with elevated 1-deoxy-SA levels. Highest levels of the 1-deoxy bases were found in G382V and I504F expressing cells; the levels in V359M expressing cells were lower, but still significantly increased in comparison to cells expressing WT SPTLC2. This finding suggests that altered SPT substrate specificity could contribute to the disease pathomechanism.

The exogenous addition of 1-deoxy-SA but not of SA has been shown to be neurotoxic to cultured primary dorsal root ganglia and, to a lesser extent, motor neurons: it impairs neurite outgrowth and induces the retraction of existing neurites, and this is associated with a disturbed actin-neurofilament interaction.[13] However, whether the

same neurotoxic mechanisms occur when 1-deoxy-SA is generated within the neuron is currently unknown. The mouse model for HSAN-I, overexpressing the SPTLC1 mutation C133W, has highly elevated levels of the atypical sphingoid bases in the sciatic nerves, whereas brain tissue is devoid of these metabolites. This is reminiscent of the pathology in HSAN-I patients, in which the peripheral nervous system is affected and the central nervous system spared, and suggests that these atypical bases could be key in disease development. Interestingly, double transgenic $SPTLC1^{WT/C133W}$ mice, overexpressing both WT and mutant SPTLC1, produce levels of 1-deoxy-SA in the sciatic nerve that are intermediary between levels in WT and $SPTLC1^{C133W}$ mice, but they do not develop a peripheral neuropathy.[32] This suggests that this metabolite is tolerated to a certain extent in the sciatic nerve. Moreover, the study of Penno et al.[13] of seven HSAN-I patients carrying the *SPTLC1* C133W mutation shows a tendency of levels for 1-deoxy-SA to be higher in patients with a more severe clinical phenotype. This is in contrast with our study, in which the levels of 1-deoxy-SA do not seem to correlate with the severity of the clinical phenotype. The patient carrying the I504F mutation and showing high 1-deoxy-SA levels presented with an atypically early onset of disease, but the patients carrying the G382V mutation, which is likewise correlated with strongly increased 1-deoxy-SA levels, had an adulthood disease onset. Possible explanations for this discrepancy could be the age of the patient, the disease stage, or the existence of hitherto unidentified genetic or environmental factors.

Sphingolipids are important structural components of eukaryotic membranes, but they are also considered to be key bioactive molecules. Together with cholesterol, they form the major constituent of the lipid rafts, regions within the plasma membrane important for cellular signaling. In neurons, they are involved in neurotrophin signaling, axon guidance, and synaptic transmission.[33] Sphingolipids and sphingoid bases are implicated in various disease processes such as cancer pathology, inflammation, and diabetes,[34,35] indicating their role in a myriad of processes in the cell. With regard to the nervous system, it is of note that mutations in a high number of enzymes involved in sphingolipid metabolism are associated with neurodegenerative diseases.[9] With this study, the importance of the sphingolipid pathway in neurological functioning is once again being stressed.

In conclusion, by using the functional candidate gene approach we identified mutations in *SPTLC2* to be associated with HSAN. Our finding extends the genetic variability in HSAN-I and enlarges the group of HSAN neuropathies associated with SPT defects. We further show that HSAN-I is consistently associated with an increased formation of the neurotoxic 1-deoxy-SA, suggesting a common pathomechanism for HSAN-I. The elucidation of 1-deoxy-SA function and HSAN-I pathology will further broaden our knowledge of the ever-expanding field of sphingolipids.

Supplemental Data

Supplemental data include one figure and three tables and can be found with this article online at http://www.cell.com/AJHG/.

Acknowledgments

We are grateful to the patients and their families for their cooperation in our research project. We thank the Genetic Service Facility (VIB) for DNA sequencing and Ilse Palmans and Deborah Seys for technical assistance with the yeast assays. This project was funded in part by a Methusalem grant of the University of Antwerp, the Fund for Scientific Research (FWO-Flanders), the Medical Foundation Queen Elisabeth (GSKE), the Association Belge contre les Maladies Neuromusculaires (ABMM), the Interuniversity Attraction Poles P6/43 program of the Belgian Federal Science Policy Office (BELSPO), and the Austrian Science Fond (FWF, P19455-B05). A.R. and J.B. are supported by Ph.D. fellowships of the Institute for Science and Technology (IWT) and FWO-Flanders, respectively. A.R. received an EMBO Short Term Fellowship. K.J. holds a postdoctoral fellowship from BELSPO. P.S. is supported by an IGA MH CR grant (no. 10552-3). Support for H.T. was provided by the German Society for Clinical Chemistry and Laboratory Medicine (DGKL), the Gebert Rüf Foundation, and the European Commission (LSHM-CT-2006-037631).

Received: July 29, 2010
Revised: September 15, 2010
Accepted: September 16, 2010
Published online: October 7, 2010

Web Resources

The URLs for data presented herein are as follows:

Clustal Multiple Sequence Alignment, http://www.clustal.org
Online Mendelian Inheritance in Man (OMIM), http://www.ncbi.nlm.nih.gov/Omim/

Accession Numbers

The GenBank accession numbers for the human SPTLC2 and SPTLC3 sequences reported in this paper are NM_004863 and NM_018327, respectively. The GenBank accession number for the LCB2 (*S. cerevisiae*) sequence is NM_001180370.

References

1. Dyck, P.J., Chance, P., Lebo, R., and Carney, J.A. (1993). Hereditary motor and sensory neuropathies. In Peripheral neuropathy, Third Edition, P.J. Dyck, P.K. Thomas, J.W. Griffin, P.A. Low, and J.F. Poduslo, eds. (Philadelphia: W.B. Saunders), pp. 1065–1093.
2. Auer-Grumbach, M. (2004). Hereditary sensory neuropathies. Drugs Today (Barc) *40*, 385–394.
3. Verpoorten, N., De Jonghe, P., and Timmerman, V. (2006). Disease mechanisms in hereditary sensory and autonomic neuropathies. Neurobiol. Dis. *21*, 247–255.
4. Bejaoui, K., Wu, C., Scheffler, M.D., Haan, G., Ashby, P., Wu, L., de Jong, P., and Brown, R.H., Jr. (2001). SPTLC1 is mutated in hereditary sensory neuropathy, type 1. Nat. Genet. *27*, 261–262.

5. Dawkins, J.L., Hulme, D.J., Brahmbhatt, S.B., Auer-Grumbach, M., and Nicholson, G.A. (2001). Mutations in SPTLC1, encoding serine palmitoyltransferase, long chain base subunit-1, cause hereditary sensory neuropathy type I. Nat. Genet. *27*, 309–312.
6. Rotthier, A., Baets, J., De Vriendt, E., Jacobs, A., Auer-Grumbach, M., Lévy, N., Bonello-Palot, N., Kilic, S.S., Weis, J., Nascimento, A., et al. (2009). Genes for hereditary sensory and autonomic neuropathies: a genotype-phenotype correlation. Brain *132*, 2699–2711.
7. Hornemann, T., Wei, Y., and von Eckardstein, A. (2007). Is the mammalian serine palmitoyltransferase a high-molecular-mass complex? Biochem. J. *405*, 157–164.
8. Hanada, K. (2003). Serine palmitoyltransferase, a key enzyme of sphingolipid metabolism. Biochim. Biophys. Acta *1632*, 16–30.
9. Kolter, T., and Sandhoff, K. (2006). Sphingolipid metabolism diseases. Biochim. Biophys. Acta *1758*, 2057–2079.
10. Dedov, V.N., Dedova, I.V., Merrill, A.H., Jr., and Nicholson, G.A. (2004). Activity of partially inhibited serine palmitoyltransferase is sufficient for normal sphingolipid metabolism and viability of HSN1 patient cells. Biochim. Biophys. Acta *1688*, 168–175.
11. Bejaoui, K., Uchida, Y., Yasuda, S., Ho, M., Nishijima, M., Brown, R.H., Jr., Holleran, W.M., and Hanada, K. (2002). Hereditary sensory neuropathy type 1 mutations confer dominant negative effects on serine palmitoyltransferase, critical for sphingolipid synthesis. J. Clin. Invest. *110*, 1301–1308.
12. Zitomer, N.C., Mitchell, T., Voss, K.A., Bondy, G.S., Pruett, S.T., Garnier-Amblard, E.C., Liebeskind, L.S., Park, H., Wang, E., Sullards, M.C., et al. (2009). Ceramide synthase inhibition by fumonisin B1 causes accumulation of 1-deoxysphinganine: a novel category of bioactive 1-deoxysphingoid bases and 1-deoxydihydroceramides biosynthesized by mammalian cell lines and animals. J. Biol. Chem. *284*, 4786–4795.
13. Penno, A., Reilly, M.M., Houlden, H., Laurá, M., Rentsch, K., Niederkofler, V., Stoeckli, E.T., Nicholson, G., Eichler, F., Brown, R.H., Jr., et al. (2010). Hereditary sensory neuropathy type 1 is caused by the accumulation of two neurotoxic sphingolipids. J. Biol. Chem. *285*, 11178–11187.
14. Rozen, S., and Skaletsky, H. (2000). Primer3 on the WWW for general users and for biologist programmers. Methods Mol. Biol. *132*, 365–386.
15. Weckx, S., De Rijk, P., Van Broeckhoven, C., and Del Favero, J. (2004). SNPbox: web-based high-throughput primer design from gene to genome. Nucleic Acids Res. *32*, W170–W172.
16. Weckx, S., Del-Favero, J., Rademakers, R., Claes, L., Cruts, M., De Jonghe, P., Van Broeckhoven, C., and De Rijk, P. (2005). novoSNP, a novel computational tool for sequence variation discovery. Genome Res. *15*, 436–442.
17. Gietz, R.D., and Schiestl, R.H. (2007). High-efficiency yeast transformation using the LiAc/SS carrier DNA/PEG method. Nat. Protoc. *2*, 31–34.
18. Dunn, T.M., Gable, K., Monaghan, E., and Bacikova, D. (2000). Selection of yeast mutants in sphingolipid metabolism. Methods Enzymol. *312*, 317–330.
19. Vandesompele, J., de Preter, K., Pattyn, F., Poppe, B., Van Roy, N., De Paepe, A., and Speleman, F. (2002). Accurate normalization of real-time quantitative RT-PCR data by geometric averaging of multiple internal control genes. Genome Biol. *3*, RESEARCH0034.
20. Rütti, M.F., Richard, S., Penno, A., von Eckardstein, A., and Hornemann, T. (2009). An improved method to determine serine palmitoyltransferase activity. J. Lipid Res. *50*, 1237–1244.
21. Riley, R.T., Norred, W.P., Wang, E., and Merrill, A.H. (1999). Alteration in sphingolipid metabolism: bioassays for fumonisin- and ISP-I-like activity in tissues, cells and other matrices. Nat. Toxins *7*, 407–414.
22. Kurth, I., Pamminger, T., Hennings, J.C., Soehendra, D., Huebner, A.K., Rotthier, A., Baets, J., Senderek, J., Topaloglu, H., Farrell, S.A., et al. (2009). Mutations in FAM134B, encoding a newly identified Golgi protein, cause severe sensory and autonomic neuropathy. Nat. Genet. *41*, 1179–1181.
23. Wang, E., Norred, W.P., Bacon, C.W., Riley, R.T., and Merrill, A.H., Jr. (1991). Inhibition of sphingolipid biosynthesis by fumonisins. Implications for diseases associated with Fusarium moniliforme. J. Biol. Chem. *266*, 14486–14490.
24. Hornemann, T., Richard, S., Rütti, M.F., Wei, Y., and von Eckardstein, A. (2006). Cloning and initial characterization of a new subunit for mammalian serine-palmitoyltransferase. J. Biol. Chem. *281*, 37275–37281.
25. Gable, K., Han, G., Monaghan, E., Bacikova, D., Natarajan, M., Williams, R., and Dunn, T.M. (2002). Mutations in the yeast LCB1 and LCB2 genes, including those corresponding to the hereditary sensory neuropathy type I mutations, dominantly inactivate serine palmitoyltransferase. J. Biol. Chem. *277*, 10194–10200.
26. Dawkins, J.L., Brahmbhatt, S.B., Auer-Grumbach, M., Wagner, K., Hartung, H.P., Verhoeven, K., Timmerman, V., De Jonghe, P., Kennerson, M.L., LeGuern, E., and Nicholson, G.A. (2002). Exclusion of serine palmitoyltransferase long chain base subunit 2 (SPTLC2) as a common cause for hereditary sensory neuropathy. Neuromuscul. Disord. *12*, 656–658.
27. Han, G., Gupta, S.D., Gable, K., Niranjanakumari, S., Moitra, P., Eichler, F., Brown, R.H., Jr., Harmon, J.M., and Dunn, T.M. (2009). Identification of small subunits of mammalian serine palmitoyltransferase that confer distinct acyl-CoA substrate specificities. Proc. Natl. Acad. Sci. USA *106*, 8186–8191.
28. Breslow, D.K., Collins, S.R., Bodenmiller, B., Aebersold, R., Simons, K., Shevchenko, A., Ejsing, C.S., and Weissman, J.S. (2010). Orm family proteins mediate sphingolipid homeostasis. Nature *463*, 1048–1053.
29. Han, S., Lone, M.A., Schneiter, R., and Chang, A. (2010). Orm1 and Orm2 are conserved endoplasmic reticulum membrane proteins regulating lipid homeostasis and protein quality control. Proc. Natl. Acad. Sci. USA *107*, 5851–5856.
30. Yard, B.A., Carter, L.G., Johnson, K.A., Overton, I.M., Dorward, M., Liu, H.T., McMahon, S.A., Oke, M., Puech, D., Barton, G.J., et al. (2007). The structure of serine palmitoyltransferase; gateway to sphingolipid biosynthesis. J. Mol. Biol. *370*, 870–886.
31. Hojjati, M.R., Li, Z., and Jiang, X.C. (2005). Serine palmitoyl-CoA transferase (SPT) deficiency and sphingolipid levels in mice. Biochim. Biophys. Acta *1737*, 44–51.
32. Eichler, F.S., Hornemann, T., McCampbell, A., Kuljis, D., Penno, A., Vardeh, D., Tamrazian, E., Garofalo, K., Lee, H.J., Kini, L., et al. (2009). Overexpression of the wild-type SPT1 subunit lowers desoxysphingolipid levels and rescues the phenotype of HSAN1. J. Neurosci. *29*, 14646–14651.
33. Tsui-Pierchala, B.A., Encinas, M., Milbrandt, J., and Johnson, E.M., Jr. (2002). Lipid rafts in neuronal signaling and function. Trends Neurosci. *25*, 412–417.
34. Zeidan, Y.H., and Hannun, Y.A. (2007). Translational aspects of sphingolipid metabolism. Trends Mol. Med. *13*, 327–336.
35. Wymann, M.P., and Schneiter, R. (2008). Lipid signalling in disease. Nat. Rev. Mol. Cell Biol. *9*, 162–176.